

Growth of Free-Standing AlN Nanocrystals on Nanorod ZnO Template*

Hu Weiguo[†], Wei Hongyuan, Jiao Chunmei, Kang Tingting, Zhang Riqing, and Liu Xianglin

(Institute of Semiconductors, Chinese Academy of Sciences, Beijing 100083, China)

Abstract: AlN film is deposited on a nanorod ZnO template by metalorganic chemical vapor deposition. Scanning electron microscopy measurements reveal that this film forms a lying nanorod surface. The grazing incidence X-ray diffraction further proves that it is entirely a wurtzite AlN structure, and the average size of the crystallite grains is about 12nm, which is near the ZnO nanorod diameter (30nm). This means that the nanorod ZnO template can restrict the AlN lateral overgrowth. Additionally, by etching the ZnO template with H₂ at high temperatures, we directly achieve epitaxial lift-off during the growth process. Eventually, free-standing AlN nanocrystals are achieved, and the undamaged area is near 1cm × 1cm. We define the growth mechanism as a “grow-etch-merge” process.

Key words: metalorganic vapor phase epitaxy; nanomaterials; nitride

EEACC: 0520F; 2520D

CLC number: O484.1

Document code: A

Article ID: 0253-4177(2007)10-1508-05

1 Introduction

Aluminum nitride (AlN) is a very promising candidate for ultraviolet optoelectronic devices, such as UV LDs, UV LEDs, and UV detectors, which are widely applied in biology, medicine, environmental detection, and high-density data storage. Because the AlN bandgap is larger than 6.2eV, these devices' quantum efficiency is predicted to be very low. Low dimensional semiconductor structures can greatly improve devices' optoelectronic performance^[1,2]. However, because AlN has a high 2D-growth velocity, it is very difficult to grow low-dimensional AlN films.

Selective area epitaxy (SAE) is a promising route for the fabrication of well-defined nanostructures. And ZnO has an important characteristic; because of its low 2D-growth velocity, ZnO easily forms a well-aligned nanorod structure with a diameter from tens of nm to hundreds of nm^[3]. Therefore, it should serve as a natural template for the SAE growth of low-dimensional AlN films.

For many novel electronic and optoelectronic

devices, epitaxial lift-off (ELO) is a key process. People have performed much research on ELO processes^[4~8]. Although laser-induced lift-off is a relatively mature process, it still has some defects: (1) It degrades the film quality and introduces more defects; and (2) It makes the fabrication process complex. ZnO has another important characteristic; it can be decomposed with H₂ at high temperatures. In particular, the ZnO nanorod structure increases the specific surface area so that the decomposition velocity is enhanced. Thus, by etching ZnO template, ELO can be achieved during growth.

To this end, we have grown AlN films on nanorod ZnO template with MOCVD. Our research reveals that this process has two distinct merits: (1) AlN nanocrystals can be obtained; (2) ELO can be achieved during the growth.

2 Experiment

First, ZnO was directly deposited on *c*-plane sapphire by MOCVD at 500°C^[3]. SEM reveals that a well-aligned nanorod-structure with a diameter of 30nm and a height of 850nm was formed.

* Project supported by the National Natural Science Foundation of China (No. 60506002)

[†] Corresponding author. Email: sivamay@semi.ac.cn

Received 7 February 2007, revised manuscript received 20 May 2007

After being diluted with deionized water, the nanorod-structure ZnO was placed into another MOCVD chamber to deposit AlN film. For comparison, a *c*-plane sapphire substrate that had been pretreated with acid was also placed into the MOCVD chamber at the same time. Then, with 6 slm pure N₂ carrier gas, a low-temperature AlN film (LT-AlN), which commonly acts as the nucleation layer for the next growth step, was deposited on these two substrates (ZnO/Sapphire and Sapphire) at 550°C for 3min. Lastly, we deposited AlN films at 1100°C for 60min. In this process, micro H₂ (0.05 slm) was introduced into the chamber to etch ZnO template. After these processes, a smooth AlN film with a thickness of about 500nm was obtained on the sapphire, which we labeled Sample A. However, the AlN film had only a weak bond with the substrate on the ZnO/Sapphire, which caused partial warping on the fringe. With a simple manual lift-off, a 1cm × 1cm free-standing AlN film was achieved, which we labeled Sample B. With no substrate, this free-standing AlN film was very fragile. If we had adopted finer lift-off technology, a larger area free-standing AlN film could have been obtained.

The surface morphologies of these samples were characterized by an FEI Sirion-200 field-emission scanning electron microscope (FE-SEM), and accessorial energy dispersive spectra (EDS) analysis was used to identify elements in the film. Grazing incidence X-ray diffraction (GIXRD) was performed to analyze the phases with an X'Pert PRO MPD, using incidence angle of 0.6°. Raman spectra were recorded using a Jobin-Yvon T64000 Raman-scattering spectrometer at room temperature in the backscattering geometry $z(x, y)\bar{z}$. The 514.5nm line of a 500mW Ar⁺ laser was used for the excitation source.

3 Results and discussion

The directly deposited ZnO formed well-aligned nanorods 30nm in diameter and 850nm in length. A surface SEM image is shown in Fig. 1 (a). In Fig. 1(b), Sample B exhibits a nanoneedle-like surface, which is just like lying nanorods, with an average diameter of about 40nm. However, in Fig. 1 (c), Sample A exhibits a smooth surface with fewer flecks. This discrepancy should be at-

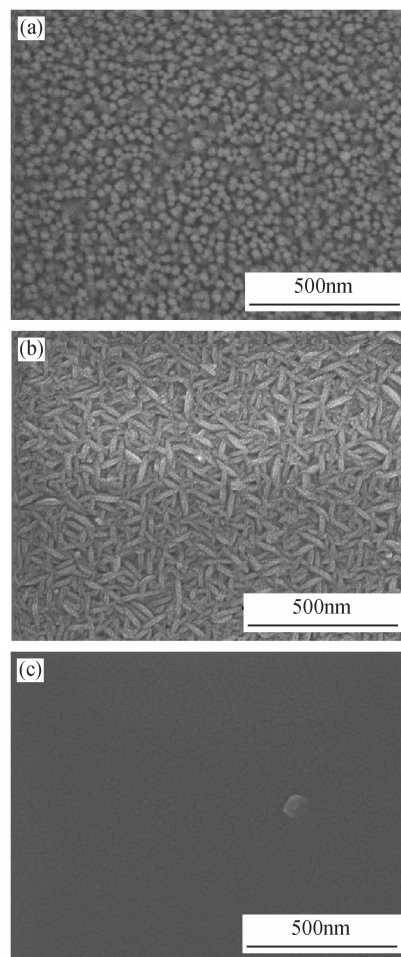


Fig.1 SEM images (a) Nanorods ZnO template; (b) Free-standing AlN nanocrystals; (c) AlN deposited on sapphire

tributed to the different growth mechanisms; the AlN deposited on sapphire was grown in a typical Wolmer-Weber-like mode, and the smooth surface and flecks correspond to merged islands and unmerged islands, respectively; however, the process of AlN deposition on ZnO/sapphire is complex, and we discuss it further below.

In Fig. 2(a), energy dispersive spectra (EDS) reveal that only Al, N, minim C, O and Au were present in Sample B, and no Zn could be detected. The C can be attributed to the decomposition of metalorganic material, and the Au arises from metal spraying in the SEM measurements. Thus, we speculate that the ZnO should have been mostly decomposed in the growth process. The Zn evaporated from the films surface, and part of the O was incorporated into Sample B. This O could combine with Al or N to form other phases, or act

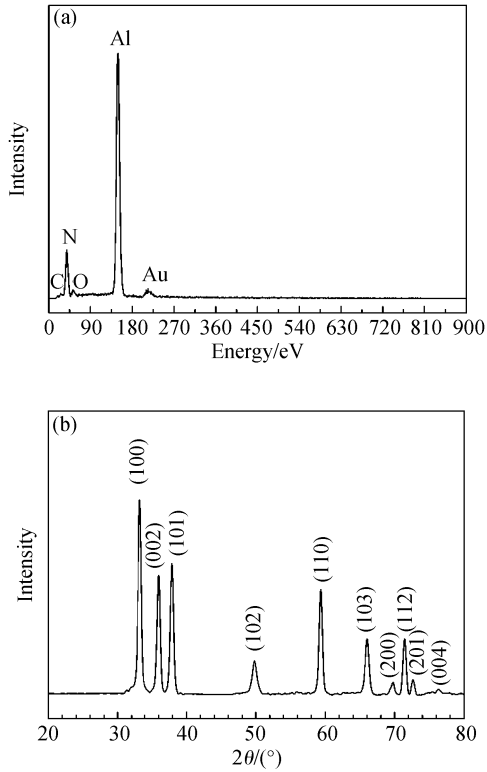


Fig.2 (a) EDS spectrum of the free-standing AlN nanocrystals; (b) SAXRD spectrum of the free-standing AlN nanocrystals. The incidence angle is 0.6° .

as an impurity. The grazing incidence X-ray diffraction reveals that the AlN is entirely a wurtzite AlN structure, as shown in Fig. 2 (b). No other phases, for example, $\text{Al}_x\text{O}_{1-x}$, $\text{Zn}_x\text{O}_{1-x}$, $\text{Zn}_x\text{Al}_y\text{O}_{1-x-y}$, $\text{Al}_x\text{N}_y\text{O}_{1-x-y}$, etc, were detected. This also demonstrates that the ZnO was mostly decomposed and the O did not form a new phase but acted as an impurity. Additionally, with the Scherrer formula, the average size of the crystallite grains is calculated to be about 12nm, which is near the ZnO nanorods' diameter (30nm). This means that the ZnO nanorod template restricts the AlN lateral overgrowth to form AlN nanocrystals.

Raman measurement results are shown in Fig. 3. Both Sample A and Sample B exhibit a clear E_2 (high) phonon mode peak. However, besides the E_2 (high) phonon mode peak, Sample B has another A_1 (TO) phonon mode peak, which cannot be observed in Sample A. This discrepancy is attributed to the polar difference between the A_1 (TO) and the E_2 (high) phonon mode; the A_1 (TO) photo mode has solely C polarization and cannot be observed along the C axis, whereas the

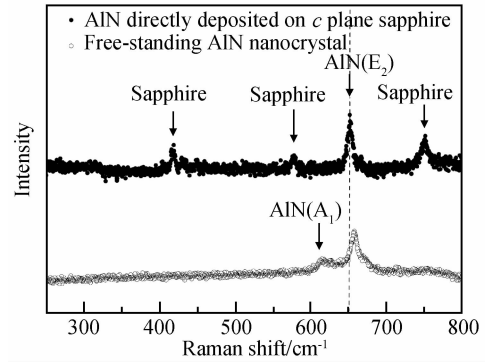


Fig.3 Raman spectra of the free-standing AlN nanocrystals and the AlN deposited on sapphire

E_2 (high) phonon mode is nonpolar^[11]. Referring to single-crystalline AlN Raman spectra at different orientations^[12], the Raman spectra of free-standing AlN nanocrystals are more similar to the spectra of $\{01\bar{1}0\}$ facet. This means that in Sample B, the nanoneedle-like surface is consisted with lying AlN nanorods, the growth orientation is along the C axis, and the lateral facet is parallel to the c-plane of sapphire.

Because the E_2 (high) phonon mode is nonpolar, it is accurate to use E_2 (high) Raman shift to calculate the stress in our experiments. The corresponding calculating formulas are listed below, and the parameters are listed in Table 1.

$$\Delta\bar{\omega}_\lambda = 2a_\lambda\varepsilon_{xx} + b_\lambda\varepsilon_{zz} = \left(2a_\lambda - \frac{2C_{13}}{C_{33}}b_\lambda\right)\varepsilon_{xx} \quad (1)$$

$$\sigma_{xx} = \left(C_{11} + C_{12} - \frac{2C_{13}^2}{C_{33}}\right)\varepsilon_{xx} \quad (2)$$

For free-strain AlN films, the frequency shift $\Delta\omega$ of the E_2 (high) phonon mode should be about 655cm^{-1} ^[10,13,14]. However, in Sample B, this $\Delta\omega$ is 657.8cm^{-1} , which corresponds to -1.10GPa compressive stress. In fact, our free-standing AlN film is warped slightly inward at the fringe, which means that the film is under compressive stress. It should be pointed out that the calculated stress value is inaccurate since we neglected the phonon confinement effect in the Raman measurements. As the microcrystal size decreases, the negative phonon dispersion relaxes the $q=0$ selection rule,

Table 1 Parameters for calculating biaxial strain

$C_{11} + C_{12}$ /Gpa	C_{13} /Gpa	C_{33} /Gpa	a_λ / cm^{-1}	b_λ / cm^{-1}	E_2 (high) $\bar{\omega}_0$ / cm^{-1}
538 ^{a)}	113 ^{a)}	370 ^{a)}	-877 ^{a)}	-911 ^{a)}	655.1 ^{b)}

a) Ref. [9]; b) Ref. [10]

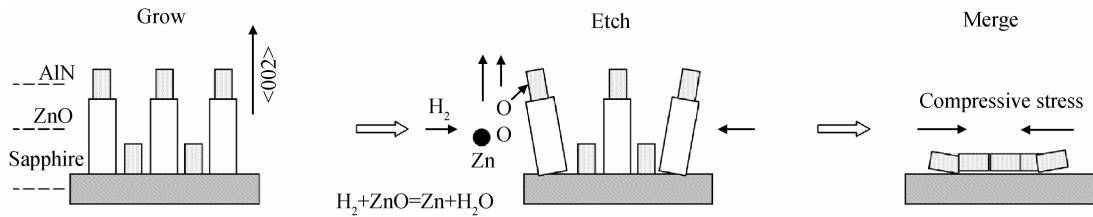


Fig. 4 Sketch map of free-standing AlN nanocrystals growth process

which makes the Raman spectrum redshift^[15,16]. However, for the free-standing AlN nanocrystals, the blueshift induced by compressive stress overwhelms the redshift effect. A similar phenomenon has also been observed in AlN nanowire deposited on sapphire^[16]. Thus, our calculated compressive stress is less than the true value. In the same growth process, Sample A exhibited a 1.5 GPa tensile stress. This means that the compressive stress cannot be attributed to AlN nucleation or epitaxy in the LT-AlN process, but arises from the mismatch between residual ZnO template and AlN nanocrystals. In the growth process, this compressive stress plays an important role; firstly, it enhances those lying nanorods merging into a film; secondly, it warps the AlN film on the fringe so that the film can be easily lifted off.

According to these studies, the growth mechanism of the freestanding AlN nanocrystals can be defined as a “grow-etch-merge” process. Figure 4 shows a simple sketch map of this process. First, when the LT AlN nucleation layer is deposited on the ZnO interlayer, AlN is uniformly grown on the ZnO template along the C axis. Since the diameter of ZnO is only 30 nm, it restricts AlN lateral overgrowth so that the AlN forms a similar nanorod structure. Secondly, with micro H_2 introduced into the chamber, ZnO nanorods slowly decompose. Zn escapes from the surface. However, minim O is still incorporated into the AlN films to act as an impurity. Due to a lack of ZnO nanorod support, the formed AlN nanorods slowly lie down. Finally, after the ZnO nanorods are decomposed, the lying AlN nanorods merge into the film under the compressive stress. Because most of the ZnO decomposed, the AlN film has a weak bond to the sapphire substrate, and the compressive stress warps the free-standing AlN nanocrystals on the fringe. Then, with a simple manual lift-off, free-standing AlN nanocrystals were achieved.

4 Conclusion

In summary, by adopting ZnO nanorods as the template, we obtained a $1\text{cm} \times 1\text{cm}$ film of free-standing AlN nanocrystals with average crystallite grains of 12 nm. We defined the growth mechanism as a “grow-etch-merge” process. Perhaps this process can be used to grow other free-standing semiconductor nanocrystal such as GaN, AlGaIn, and InN.

References

- [1] Fafard S, Hinzer K, Raymond S, et al. Red-emitting semiconductor quantum dot lasers. *Science*, 1996, 274: 5291
- [2] Devoret M H, Schoelkopf R J. Amplifying quantum signals with the single-electron transistor. *Nature*, 2000, 406: 6799
- [3] Cong G W, Wei H Y, Zhang P F, et al. One-step growth of ZnO from film to vertically well-aligned nanorods and the morphology-dependent Raman scattering. *Appl Phys Lett*, 2005, 87: 231903
- [4] Yablonovitch E, Gmitter T, Harbison J P, et al. Extreme selectivity in the lift-off of epitaxial GaAs films. *Appl Phys Lett*, 1987, 51: 2222
- [5] Hasko D G, Cleaver J R A, Ahmed H, et al. Hopping conduction in a freestanding GaAs-AlGaAs heterostructure wire. *Appl Phys Lett*, 1993, 62: 2533
- [6] Wong W S, Sands T, Cheung N W. Damage-free separation of GaN thin films from sapphire substrates. *Appl Phys Lett*, 1998, 72: 599
- [7] Wong W S, Sands T, Cheung N W, et al. Fabrication of thin-film InGaIn light-emitting diode membranes by laser lift-off. *Appl Phys Lett*, 1999, 75: 1360
- [8] Haberer E D, Sharma R, Meier C, et al. Free-standing, optically pumped, GaN/InGaIn microdisk lasers fabricated by photoelectrochemical etching. *Appl Phys Lett*, 2004, 85: 5179
- [9] Wager J M, Bechstedt F. Phonon deformation potentials of α -GaN and -AlN: an *ab initio* calculation. *Appl Phys Lett*, 2000, 77: 346
- [10] Tischler J G, Freitas J A. Anharmonic decay of phonons in strain-free wurtzite AlN. *Appl Phys Lett*, 2004, 85: 1943
- [11] Bergman L, Dutta M, Balkas C, et al. Raman analysis of the E1 and A1 quasi-longitudinal optical and quasi-transverse optical modes in wurtzite AlN. *J Appl Phys*, 1999, 85: 3535
- [12] Bickermann M, Epelbaum B M, Heimann P, et al. Orientation-dependent phonon observation in single-crystalline aluminum nitride. *Appl Phys Lett*, 2005, 86: 131904

- [13] Bergman L, Alexson D, Murphy P L, et al. Raman analysis of phonon lifetimes in AlN and GaN of wurtzite structure. *Phys Rev B*, 1999, 59: 12977
- [14] Goni A R, Siegle H, Syassen K, et al. Effect of pressure on optical phonon modes and transverse effective charges in GaN and AlN. *Phys Rev B*, 2001, 64: 35205
- [15] Tananka A, Qnari S, Arai T. Raman scattering from CdSe microcrystals embedded in a germanate glass matrix. *Phys Rev B*, 1992, 45: 6587
- [16] Zhao Qing, Zhang Hongzhou, Xu Xiang, et al. Optical properties of highly ordered AlN nanowire arrays grown on sapphire substrate. *Appl Phys Lett*, 2005, 86: 193101

用纳米棒 ZnO 作模板生长无支撑的 AlN 纳米晶*

胡卫国[†] 魏鸿源 焦春美 康亭亭 张日清 刘祥林

(中国科学院半导体研究所, 北京 100083)

摘要: 用金属有机物气相外延在纳米棒 ZnO 模板上沉积 AlN 薄膜. SEM 测试表明该薄膜形成了一种倾倒纳米棒的表面. 而 GIXRD 测试进一步证实它是纤锌矿结构的 AlN, 晶粒尺度约为 12nm, 接近于 ZnO 纳米棒的直径 (30nm). 这意味着纳米棒结构的 ZnO 能限制 AlN 的横向生长. 此外, 高温下用 H₂ 刻蚀 ZnO 直接在生长中实现了外延层的剥离. 最终得到了无支撑的 AlN 纳米晶, 完整无破损的区域约为 1cm × 1cm. 定义这个生长机制为“生长-刻蚀-合并”过程.

关键词: 金属有机物气相外延; 纳米材料; 氮化物

EEACC: 0520F; 2520D

中图分类号: O484.1

文献标识码: A

文章编号: 0253-4177(2007)10-1508-05

* 国家自然科学基金资助项目 (批准号: 60506002)

[†] 通信作者. Email: sivamay@semi.ac.cn

2007-02-07 收到, 2007-05-20 定稿